Unique Microstructure of Mesoporous Pt (H_I-Pt) Prepared via Direct Physical Casting in Lyotropic Liquid Crystalline Media

Yusuke Yamauchi,[†,‡] Toshiyuki Momma,[‡,||] Minekazu Fuziwara,[§] Sivakumar Sadasivan Nair,[||] Tetsu Ohsuna,[⊥] Osamu Terasaki,[⊥] Tetsuya Osaka,[†,‡,§] and Kazuyuki Kuroda*[,†,‡,§,||]

Department of Applied Chemistry and Major in Nanoscience & Nanoengineering, Faculty of Science & Engineering, Waseda University, Ohkubo-3, Shinjuku-ku, Tokyo 169-8555, Japan, Kagami Memorial Laboratory for Materials Science & Technology, Waseda University, Nishiwaseda-2, Shinjuku-ku, Tokyo 169-0051, Japan, CREST, Japan Science and Technology Agency, 4-1-8, Honcho, Kawaguchi-shi Saitama 332-0021, Japan, and Department of Structural Chemistry, Arrhenius Laboratory, Stockholm University, Stockholm S-10691, Sweden

Received August 16, 2005. Revised Manuscript Received October 5, 2005

Two-dimensional hexagonally ordered mesoporous Pt particles are prepared by Pt deposition in the aqueous domains of lyotropic liquid crystals (LLC) by chemical reduction with Zn powders. Interestingly, the framework is composed of connected nanoparticles of about 3 nm in size. Moreover, it is proved that the lattice fringes on the atomic crystallinity are coherently extended across the several nanoparticles in the framework. Such a framework composed of connected nanoparticles with extended crystallinity is uniquely created by using LLC as a soft template, which is not attainable by a traditional approach using mesoporous silica as a hard template. Through the structural identification, the formation mechanism of mesoporous Pt in the presence of LLC is thought to be continuous deposition of Pt nanoparticles from one nanoparticle.

Introduction

Metal-based nanoarchitectured materials are of great importance for new developments of many applications including electrodevices, magnetic recording media, optical devices, and metal catalysts. Structural nanoscale design is one of the important key issues in bottom-up nanotechnology. Since the first discovery of mesoporous silica,[1] the self-assembly of surfactants has been well-recognized as a powerful tool for templated synthesis of mesoporous materials[2] and has created a great avenue for the production of many types of metal-based nanomaterials including nanoparticles,[3] nanowires,[4] and 3D networks.[5] These metal-based nanomaterials have mainly been prepared from various mesoporous silicas (e.g., FSM-16, MCM-41, MCM-48, SBA-15, and HMM-1) as hard templates.[3−5]

Currently, lyotropic liquid crystals (LLC) made of nonionic surfactant at a high concentration have been introduced as a soft template. Since the first report,[6] many mesoporous metals have been successfully prepared through direct physical casting from a H_I (2D hexagonal) mesophase of LLC media.[7] Mesoporous metals possess a *p6 mm* mesostructure, namely, a regular 2D hexagonal array of cylindrical mesochannels, which is not achievable by the previous methods using mesoporous silica as a hard template. Although direct physical casting is a simple approach and can be readily

* To whom correspondence should be addressed: phone/fax +81-3-5286-3199; e-mail kuroda@waseda.jp.

† Department of Applied Chemistry, Waseda University.

‡ Major in Nanoscience & Nanotechnology, Waseda University.

§ Kagami Memorial Laboratory for Materials Science and Technology, Waseda University.

|| CREST, Japan Science and Technology Agency.

⊥ Department of Structural Chemistry, Stockholm University.

(1) Yanagisawa, T.; Shimizu, T.; Kuroda, K.; Kato, C. *Bull. Chem. Soc. Jpn.* **1990**, *63*, 988−992.

(2) (a) Kresge, C. T.; Leonowicz, M. E.; Roth, W. J.; Vartuli, J. C.; Beck, J. S. *Nature* **1992**, *359*, 710−712. (b) Inagaki, S.; Fukushima, Y.; Kuroda, K. *J. Chem. Soc., Chem. Commun.* **1993**, 680−682. (c) Monnier, A.; Schüth, F.; Huo, Q.; Kumar, D.; Margolese, D.; Maxwell, R. S.; Stucky, G. D.; Krishnamurty, M.; Petroff, P.; Firouzi, A.; Janicke, M.; Chmelka, B. F. *Science* **1993**, *261*, 1299−1303. (d) Huo, Q. S.; Margolese, D. I.; Ciesla, U.; Feng, P. Y.; Gier, T. E.; Sieger, P.; Leon, R.; Petroff, P. M.; Schüth, F.; Stucky, G. D. *Nature* **1994**, *368*, 317−321. (e) Bagshaw, S. A.; Prouzet, E.; Pinnavaia, T. J. *Science* **1995**, *269*, 1242−1244. (f) Attard, G. S.; Glyde, J. C.; Göltner, C. G. *Nature* **1995**, *378*, 366−368. (g) Sakamoto, Y.; Kaneda, M.; Terasaki, O.; Zhao, D. Y.; Kim, J. M.; Stucky, G. D.; Shim, H. J.; Ryoo, R. *Nature* **2000**, *408*, 449−453. (h) Che, S.; Liu, Z.; Ohsuna, T.; Sakamoto, K.; Terasaki, O.; Tatsumi, T. *Nature* **2004**, *429*, 281−284.

(3) (a) Fukuoka, A.; Higashimoto, N.; Sakamoto, Y.; Inagaki, S.; Fukushima, Y.; Ichikawa, M. *Top. Catal.* **2002**, *18*, 73−78. (b) Fukuoka, A.; Araki, H.; Kimura, J.; Sakamoto, Y.; Higuchi, T.; Sugimoto, N.; Inagaki, S.; Ichikawa, M. *J. Mater. Chem.* **2004**, *14*, 752−756.

(4) (a) Ko, C. H.; Ryoo, R. *Chem. Commun.* **1996**, 2467−2468. (b) Liu, Z.; Sakamoto, Y.; Ohsuna, T.; Hiraga, K.; Terasaki, O.; Ko, C. H.; Shin, H. J.; Ryoo, R. *Angew. Chem., Int. Ed.*, **2000**, *39*, 3107−3110. (c) Liu, Z.; Terasaki, O.; Ohsuna, T.; Hiraga, K.; Shin, H. J.; Ryoo, R. *Chem. Phys. Chem.* **2001**, *2*, 229−231. (d) Fukuoka, A.; Sakamoto, Y.; Guan, S.; Inagaki, S.; Sugimoto, N.; Fukushima, Y.; Hirahara, K.; Iijima, S.; Ichikawa, M. *J. Am. Chem. Soc.* **2001**, *123*, 3373−3374. (e) Terasaki, O.; Liu, Z.; Ohsuna, T.; Shin, H. J.; Ryoo, R. *Microsc. Microanal.* **2002**, *8*, 35−39. (f) Sakamoto, Y.; Fukuoka, A.; Higuchi, T.; Shimomura, N.; Inagaki, S.; Ichikawa, M. *J. Phys. Chem. B* **2004**, *108*, 853−858. (g) Yue, B.; Tang, H. L.; Kong, Z. P.; Zhu, K.; Dickinson, C.; Zhou, W. Z.; He, H. Y. *Chem. Phys. Lett.* **2005**, *407*, 83−86.

(5) (a) Shin, H. J.; Ryoo, R.; Liu, Z.; Terasaki, O. *J. Am. Chem. Soc.* **2001**, *123*, 1246−1247. (b) Choi, K. S.; McFarland, E. W.; Stucky, G. D. *Adv. Mater.* **2003**, *15*, 2018−2021. (c) Guo, X. J.; Yang, C. M.; Liu, P. H.; Cheng, M. H.; Chao, K. J. *Cryst. Growth Des.* **2005**, *5*, 33−36.

(6) Attard, G. S.; Göltner, C. G.; Corker, J. M.; Henke, S.; Templer, R. H. *Angew. Chem., Int. Ed. Engl.* **1997**, *36*, 1315−1317.

10.1021/cm051844q CCC: $30.25
Published on Web 11/12/2005

applied to the preparation of many mesoporous metals in a wide range of metal species, mesoporous/mesostructured metals reported so far are less ordered in almost all cases than those reported for mesoporous inorganic oxides including silica. This is because LLC media as a template are viscous and the rodlike self-assemblies (rods) are flexible. The careful control of metallization in the aqueous domains of LLC media is a very important factor for the formation of high-quality mesostructure.[8] We have previously shown the formation of highly ordered mesoporous Ni[9] and mesostructured Ni−Co alloy[10] particles by applying an autocatalytic deposition under controlled bath conditions. Through the direct TEM observations of highly ordered mesoporous Ni metals, it has been very recently clarified that the arrangements of rods in LLC indeed work as a scaffold to direct the grain growth of Ni. The Ni mesostructures have macroscopic alignments derived from those of LLC media.[11]

We consider that LLC with high viscosity are the confined reaction media for metal deposition. The LLC media should be soft templates, and the environment for the nanoscale metal deposition is very different from that inside the mesochannels of mesoporous silica. The high-resolution scanning electron microscopic (HR-SEM) images reported previously in our systematic studies have suggested that the frameworks of mesoporous metals are composed of nanoparticles and that the morphology does not show a smooth surface.[9−11] Although many types of mesoporous metals with various compositions have been prepared to date, both nanoscale morphology and atomic-scale crystallinity of the framework of the mesoporous metals prepared from LLC have not been clarified at all. Herein we report for the first time the detailed microstructure of 2D hexagonally ordered mesoporous Pt particles (abbreviated as meso-Pt) deposited in the presence of LLC media. The framework and atomic crystallinity of meso-Pt have been fully characterized by UHR (ultrahigh resolution)-SEM and transmission electron microscopy (TEM). The interesting surface structures of the framework with connected nanoparticles were clarified and the atomic-scale Pt crystallinity in the framework was confirmed. Accurate structural information on mesoporous metals must contribute to the new development of mesoporous metals toward the superior physical and chemical properties.

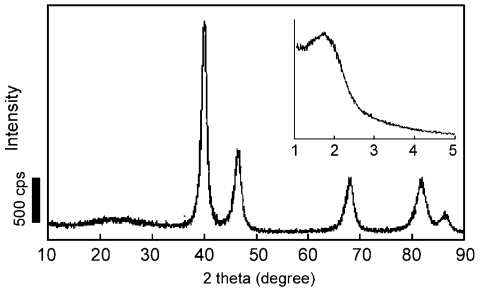

Figure 1. Powder XRD pattern of mesoporous Pt(Cu Kα). Inset: Pattern in the low-angle region (Fe Kα).

Experimental Section

Preparation of 2D-Hexagonally Ordered Meso-Pt. Two-dimensional hexagonnally ordered meso-Pt was prepared by modifying the procedure reported elsewhere.[6,12] The LLC templating mixture for the preparation of meso-Pt was composed of ternary systems: 29 wt % Pt salts [hydrogen hexachloroplatinate(IV) hydrate, HCPA, Alfa], 29 wt % deionized water, and 42 wt % nonionic surfactant ($C_{16}EO_8$, Aldrich). At first, HCPA was dissolved in deionized water. Then $C_{16}EO_8$ as a LLC former was added into the solution, and the mixture was stirred vigorously with a plastic spatula. After the mixing, the mixture was sealed in a vial and subjected to three heating (up to 80 °C)/cooling (down to 20 °C) cycles, and then the mixture was allowed to stand at 40 °C for 30 h. The use of a sealed case can suppress the evaporation of water molecules, which may affect the structures of LLC mesophases. This aging time produced a long-range ordering of LLC mesophase, which plays a key role for the preparation of highly ordered meso-Pt. The Pt complexes in the LLC phases were reduced by adding large pieces of metallic Zn, and the mixture was allowed to stand at 40 °C for 12 h until the mixture became fully black. The black products after the chemical reduction were washed successively with ethanol, water, hydrochloric acid (6 M), water, and ethanol. Ethanol was used to remove the templates, and hydrochloric acid was used to dissolve Zn pieces left in the LLC templating mixture.

Characterization. Powder XRD patterns in the range of low diffraction angles were recorded by using a Mac Science M03XHF22 diffractometer with Mn-filtered Fe Kα radiation (40 kV, 20 mA) at a scanning rate of 0.5°/min, while those in the range of high angles were obtained by a Rigaku Rint 2500X diffractometer with monochromated Cu Kα radiation (40 kV, 100 mA) operated by using a step scan program (step width 0.05°). SEM images were obtained by a Hitachi HR-SEM S-5500 microscope. Powder samples without coating were observed directly. TEM images were obtained by a JEOL JEM-2010 transmission electron microscope operated at an accelerating voltage of 200 kV. Powder samples for the TEM measurement were dispersed in ethanol and mounted on a microgrid. Nitrogen adsorption and desorption isotherms were obtained by using a Belsorp 28 apparatus (Bel Japan, Inc.) at 77 K. Samples were heated at 100 °C for 3 h before the measurement.

Results and Discussion

The low-angle XRD pattern (Fe Kα radiation) of meso-Pt showed a single broad diffraction peak in the range of $1° < 2\theta < 3°$ (Figure 1, inset). The SEM image revealed that meso-Pt showed spherical morphology with a very broad size distribution (Figure 2a). The HR-SEM images of the

(7) (a) Attard, G. S.; Bartlett, P. N.; Coleman, N. R. B.; Elliott, J. M.; Owen, J. R.; Wang, J. H. *Science* **1997**, *278*, 838−840. (b) Whitehead, A. H.; Elliott, J. M.; Owen, J. R.; Attard, G. S. *Chem. Commun.* **1999**, 331−332. (c) Nelson, P. A.; Elliott, J. M.; Attard, G. S.; Owen, J. R. *Chem. Mater.* **2002**, *14*, 524−529. (d) Jiang, J. H.; Kucernak, A.; *Chem. Mater.* **2004**, *16*, 1362−1367. (e) Luo, H. M.; Sun, L.; Lu, Y. F.; Yan, Y. S. *Langmuir* **2004**, *20*, 10218−10222. (f) Boo, H.; Park, S.; Ku, B. Y.; Kim, Y.; Park, J. H.; Kim, H. C.; Chung, T. D. *J. Am. Chem. Soc.* **2004**, *126*, 4524−4525.

(8) (a) Elliott, J. M.; Attard, G. S.; Bartlett, P. N.; Coleman, N. R. B.; Merckel, D. A. S.; Owen, J. R. *Chem. Mater.* **1999**, *11*, 3602−3609. (b) Yamauchi, Y.; Yokoshima, T.; Momma, T.; Osaka, T.; Kuroda, K. *Chem. Lett.* **2004**, *33*, 1576−1577.

(9) (a) Yamauchi, Y.; Yokoshima, T.; Mukaibo, H.; Tezuka, M.; Shigeno, T.; Momma, T.; Osaka, T.; Kuroda, K. *Chem. Lett.* **2004**, *33*, 542−543. (b) Yamauchi, Y.; Momma, T.; Yokoshima, T.; Kuroda, K.; Osaka, T. *J. Mater. Chem.* **2005**, *15*, 1987−1994.

(10) (a) Yamauchi, Y.; Yokoshima, T.; Momma, T.; Osaka, T.; Kuroda, K. *J. Mater. Chem.* **2004**, *14*. 2935−2940. (b) Yamauchi, Y.; Sadasivan Nair, S.; Yokoshima, T.; Momma, T.; Osaka, T.; Kuroda, K. *Stud. Surf. Sci. Catal*. **2005**, *156*, 457−464.

(11) Yamauchi, Y.; Yokoshima, T.; Momma, T.; Osaka, T.; Kuroda, K. *Electrochem. Solid-State. Lett.* **2005**, *8*, C141−C144.

(12) (a) Jiang, J.; Kucernak, A. *J. Electroanal. Chem.* **2002**, *520*, 64−70. (b) Jiang, J.; Kucernak, A. *J. Electroanal. Chem.* **2002**, *533*, 153−165. (c) Jiang, J.; Kucernak, A. *J. Electroanal. Chem.* **2003**, *543*, 187−199. (d) Kucernak, A.; Jiang, J. *Chem. Eng. J.* **2003**, *93*, 81−91.

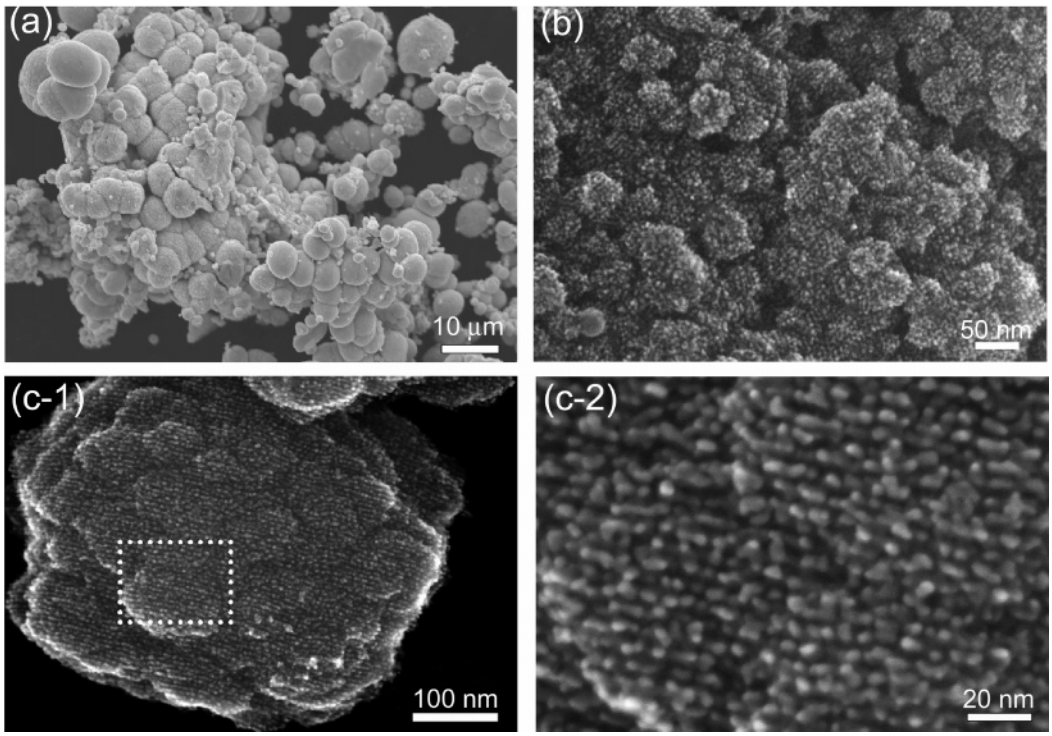

Figure 2. HR-SEM images of (a) the morphology of mesoporous Pt particles, (b) 2D hexagonal arrangements of mesopores on the external surface of mesoporous Pt particles, (c-1) running mesochannels on the external surface, and (c-2) highly magnified image of the selected area in panel c-1.

external surfaces showed the presence of both 2D hexagonally arranged mesopores and the uniform arrays of mesochannels (Figure 2b,c-1). The image analysis gives the pore diameter in the range of 3.0 ± 0.2 nm and the thickness of the pore wall to be 3.0 ± 0.2 nm, and then the pore−pore distance is found to be ca. 6 nm.

The broad diffraction in the low-angle XRD pattern is in clear contrast to the highly ordered regular mesostructure observed in the HR-SEM images. The reason why the low-angle peak is broadened can be explained by the following two factors. One possibility is the overlapping of many slightly different peaks, resulting in the broadening. The SEM and TEM images (Figures 2c-2 and 3a) hint that the size of Pt nanoparticles forming the framework varies and correspondingly the distances among mesopores are also variable. Therefore, the periodicity of the mesostructure should be slightly different for each particle. This situation may also occur even within one particle. In fact, Attard and coworkers[8a] have reported that the pore−pore distance of a mesostructure is changed depending on the bath conditions, such as bath temperature, deposition potential, and so on. In the present system, Zn powders are used by an electron source. Accordingly, the deposition potential should be different by the distance between reaction sites and Zn powders in the LLC templating mixture. Another possibility is the broadening induced by the short coherence length of single mesoporous crystallinity. In fact, many defects are present in a mesoporous structure as observed in Figure 2c-2, even though the mesochannels in one particle of about 300 nm in size seem to be aligned in the same direction (Figure 2c-1). Therefore, the domain size regarded as single mesoporous crystallinity must be much smaller than expected.

The mesopores observed at the external surface are open, providing a pathway for good diffusion. The specific surface area measured by a BET method was determined to be ca. 65 m^2/g, and this value is larger than that of commercial Pt black (20−40 m^2/g). Up to date, the surface areas of mesoporous metals including Pt have been evaluated by the BET method, which has commonly been applied to zeolites and mesoporous silica. To calculate the surface area of mesoporous Pt films or particles, the electrochemical method (e.g., cyclic voltammogram in an aqueous H_2SO_4 solution) has recently been applied due to its merit of proving the catalytic activity of the surface instead of the physical surface area evaluated by the BET method. The active area calculated by the electrochemical method is in agreement with the physical surface area evaluated by BET, as has already been reported.[12,13] Therefore, we consider that the BET method can be used for calculation of the specific surface area of mesoporous metals, in particular mesoporous Pt.

We investigated further the detailed microstructure of the framework at higher magnification (Figure 2c-2). Interestingly, the framework composed of connected nanoparticles with an average size of ca. 3 nm (bright area) and mesochannels (dark region) are clearly observed. The TEM image also provides evidence of the presence of connected nanoparticles in the framework (Figure 3a).

Two types of TEM images, with the incident electron beam perpendicular (Figure 3b-1) and parallel (Figure 3c) to the direction of main channels, were taken from the edges of meso-Pt exhibiting mesoporous structures. Surprisingly,

(13) (a) Evans, S. A. G.; Elliott, J. M.; Andrews, L. M.; Bartlett, P. N.; Doyle, P. J.; Denuault, G. *Anal. Chem.* **2002**, *74*, 1322−1326. (b) Park, S.; Chung, T. D.; Kim, H. C. *Anal. Chem.* **2003**, *75*, 3046−3049.

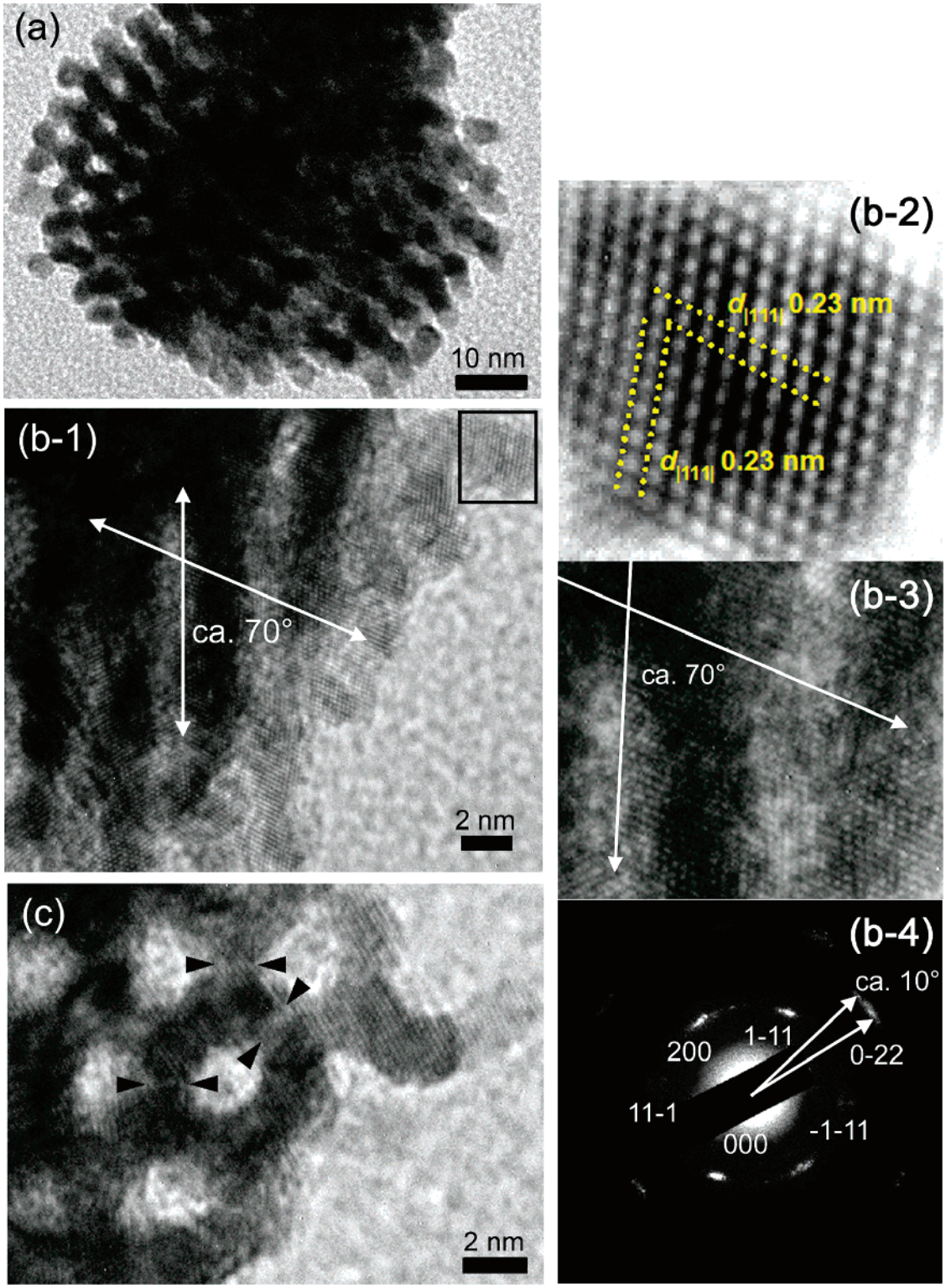

Figure 3. (a) TEM images of the morphology of mesoporous Pt particles. (b-1, c) Highly magnified TEM images with the incident electron beam perpendicular (b-1) and parallel (c) to the direction of main channels. (b-2) Filtered image of the square area in panel b-1. (b-3) Enlarged view of the dihedral angle. (b-4) Electron diffraction pattern of the selected area.

it is proved that the lattice fringes extend coherently across several nanoparticles, despite the bumpy morphology (Figure 3b-1). The lattice fringes, as indicated by the square, correspond to the {111} planes of Pt because both *d* spacings are 0.23 nm and the dihedral angle is ca. 70° (Figure 3b-2). Moreover, the dihedral angle, as indicated by the arrows, between the two lattice fringes running over the larger area is also estimated to be ca. 70°, retaining the same single crystallinelike state (Figure 3b-1,b-3). The selected-area ED pattern from a 100 nm region showed the main spots with arcs indexed to be 111 and 200 reflections of fcc Pt (Figure 3b-4). The width of the arcs can be measured to be about 10°. Consequently, the selected area possesses the atomic arrangements of Pt fcc close to a "single crystal state". Furthermore, the lattice fringes run in the same direction across the 2D hexagonally ordered mesopores (Figure 3c).

Scheme 1. Suggested Mechanism for Pt Deposition in the Aqueous Domain of the Lyotropic Liquid Crystalline Media

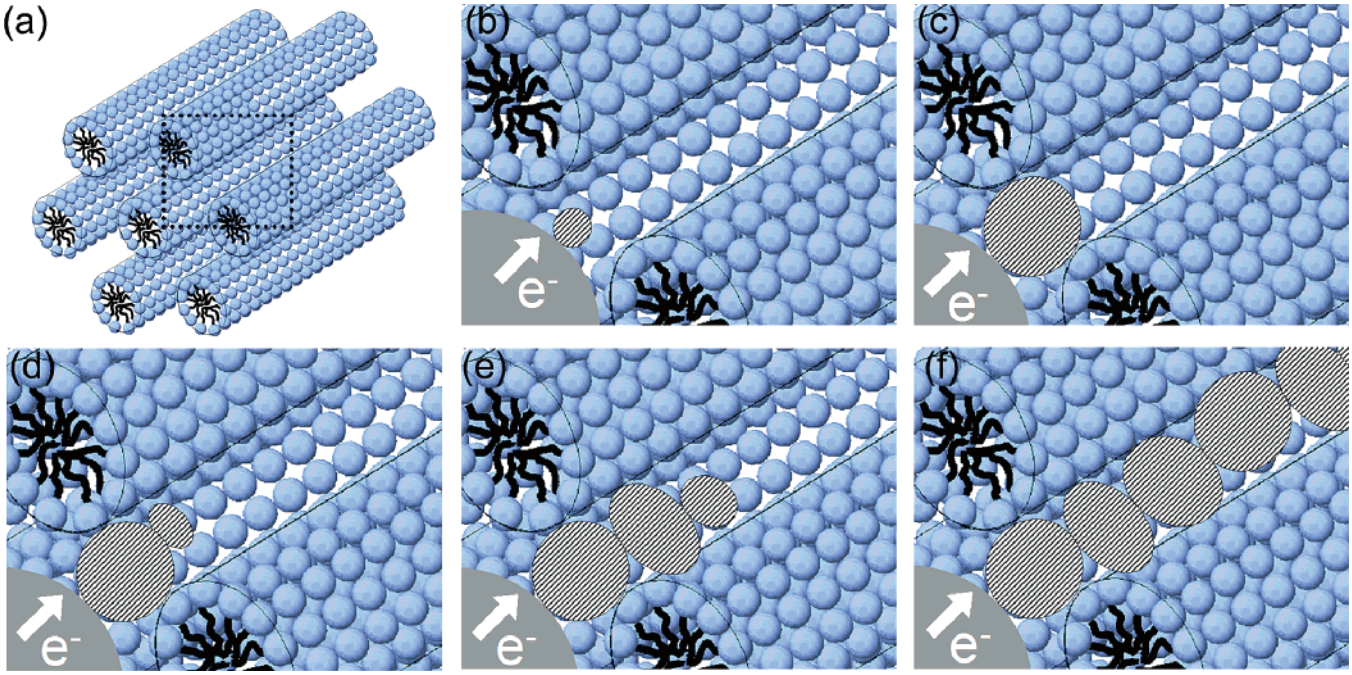

Thus, it can be regarded that the mesopores exist in a single crystallike domain. Additionally, the powder X-ray diffraction profile in the wide-angle (Cu Kα radiation) shows the (111), (200), (220), (311), and (222) diffraction peaks assigned to the Pt fcc structure, which is evidence that the whole area of the samples has the Pt fcc atomic arrangement (Figure 1).

The formation of the unique framework with a good atomic crystallinity can reasonably be explained by the following suggested mechanism (Scheme 1). The mechanism is mainly classified into three steps. (1) Primary nucleation (stage a∼b). An aqueous domain, a free space among rods, is nanoscale reaction media for the metal deposition (stage a). Initially, a primary cluster of metal atoms (Pt_0) is formed by the first reduction (stage b).[6,14] (2) Isotropic grain growth from the primary cluster (stage b∼c). In the aqueous domain, the primary Pt cluster would isotropically grow into a sphere to minimize the surface energy of the Pt grain (stage b∼c). (3) Formation of a bumpy Pt framework (stage c∼f). The bumpy morphology of the framework is a unique feature created from the LLC media as a soft template. The growing grain dislodges both water and ethylene oxide groups in the aqueous domain, because rods made of nonionic surfactants are mobile (stage c). The isotropic grain growth is hindered by the 2D hexagonally ordered rods (stage c) to produce the stress against the rods. Then, the rods are slightly distorted and undergo a plastic deformation. The grown nanoparticle would be fitted and stabilized among the rods (stage c). Therefore, as the Pt deposition proceeds, the isotropic growth of the second nanoparticle should start from the next primary nucleus formed by transferred electrons (stage d). The highly magnified TEM image (Figure 3b-1) of meso-Pt shows that the Pt fcc crystallinity is extended coherently across several nanoparticles. Therefore, it is indicated that the second Pt nanoparticle is really formed from another nucleus generated on the external surface of the first Pt nanoparticle, retaining the single crystallinelike state (stage d). Furthermore, the retention may be affected by both restricted diffusion of Pt species in a confined space and interfacially directed growth on rods, as has been reported for Pt nanodendrimers on ribosome surfaces.[15] The present system using Zn powders[12] may provide enough overvoltage for the generation of Pt nuclei on the external surface of Pt nanoparticles (stage d). This formation mechanism can explain the continuous connection of Pt nanoparticles to give the bumpy Pt frameworks (stage e∼f), and further experiments on other metals will confirm this unusual mechanism.

The Pt deposition was performed with transferred electrons created by dissolving Zn powders, that is, the reaction starts from only the external surfaces of Zn powders. In the present system, the connected Pt nanoparticles deposited on one Pt nanoparticle should possess the atomic arrangements aligned in almost the same direction. Although Scheme 1 displays only the Pt deposition along the rods, the continuous formation of Pt nanoparticles should proceed in some directions to make mesostructures (Scheme 2a). This is supported by the fact that the lattice fringes running across mesopores can also be observed, as shown in Figure 3c. This Pt deposition is a sort of positive−negative relation with the one-dimensional Pt deposition along mesochannels of mesoporous (*p6 mm*) silica. Zn^{2+} ions should be generated in the aqueous domains of the LLC during the Pt deposition. The concentration of Zn^{2+} ions must be increased with the deposition time, while that of Pt complexes must be decreased. Such a change of composition should locally occur, because the Pt deposition starts from the external

(14) Kijima, T.; Yoshimura, T.; Uota, M.; Ikeda, T.; Fujikawa, D.; Mouri, S.; Uoyama, S. *Angew. Chem., Int. Ed.* **2003**, *43*, 228−232.

(15) (a) Song, Y. J.; Yang, Y.; Medforth, C. J.; Pereira, E.; Singh, A. K.; Xu, H. F.; Jiang, Y. B.; Brinker, C. J.; van Swol, F.; Shelnutt, J. A. *J. Am. Chem. Soc.* **2004**, *126*, 635−645. (b) Polleux, J.; Pinna, N.; Antonietti, M.; Niederberger, M. *Adv. Mater.* **2004**, *16*, 436−439.

Scheme 2. Zn and SBH Systems[a]

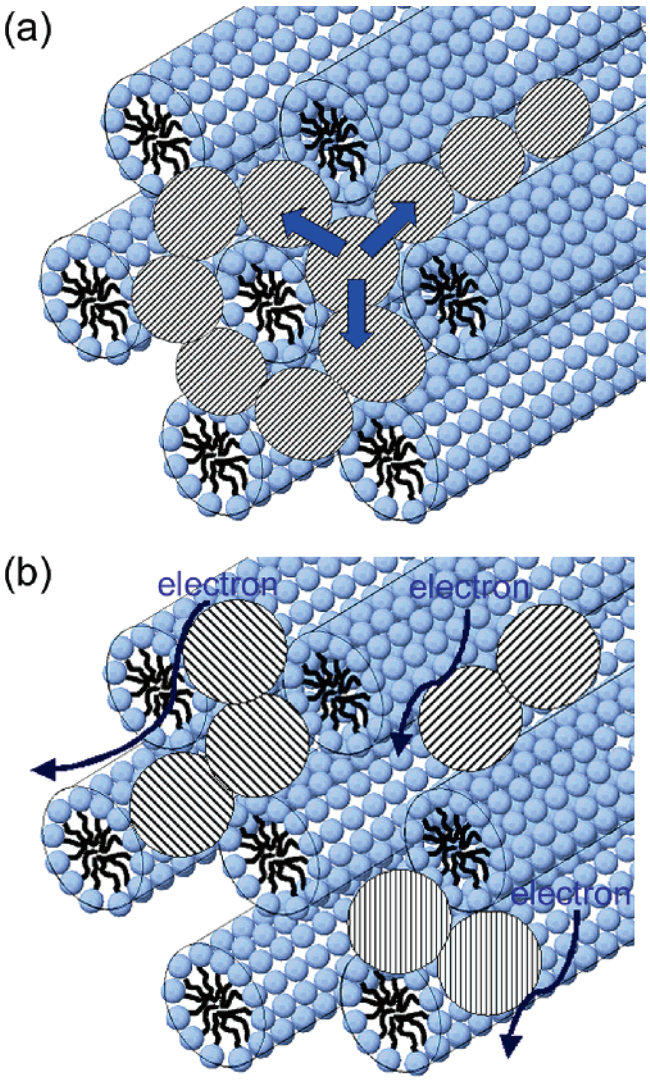

[a] (a)The Zn system shows continuous growth of Pt nanoparticles from one nanoparticle. Arrows indicate the growth direction of Pt nanoparticles. (b) The SBH system shows formation of a large amount of nuclei by self-decomposition reaction of SBH molecules.

surface of Zn powders. Although such a change of composition may induce a collapse or a phase separation of well-ordered LLC mesophase,[16] the mesoporous Pt particles obtained here have a well-ordered 2D hexagonal structure. Therefore, the structure of the LLC mesophase must be well retained during the deposition process, and the change of compositions does not affect the change of LLC mesophase in this case.

This situation by Zn is basically different from the metal deposition by simultaneous multiple nucleation, for example, the preparation of dispersed metal nanoparticles by use of SBH (sodium borohydride).[17] For comparison, Pt was deposited from the same LLC templating mixture with SBH as a reducing agent. From TEM observations, the spherical particles with a disordered porous nanostructure were mainly observed (Figure 4a). It should be noted that lattice fringes in the framework were randomly oriented (Figure 4b). This means that a large amount of nuclei all over the LLC were instantaneously created by self-decomposition reaction of SBH molecules. Therefore, Pt cannot be deposited along the rods at all to make a disordered mesoporous structure (Scheme 2b). From the above results, the continuous formation of Pt nanoparticles from one particle (Scheme 2a) plays an important role for the high quality of mesostructure.

The aqueous space between two rods is smaller than that among three rods, which may induce a different confined degree in the reaction media for the Pt deposition. In other words, the former space would give more confined environment for the Pt deposition to form smaller Pt nanoparticles, which seems to be indicated by a little fainter density, as shown by the triangles in the TEM image (Figure 3c). It hints that the size of Pt nanoparticles in the framework is slightly changed by the confined degree, although this should be investigated further in future.

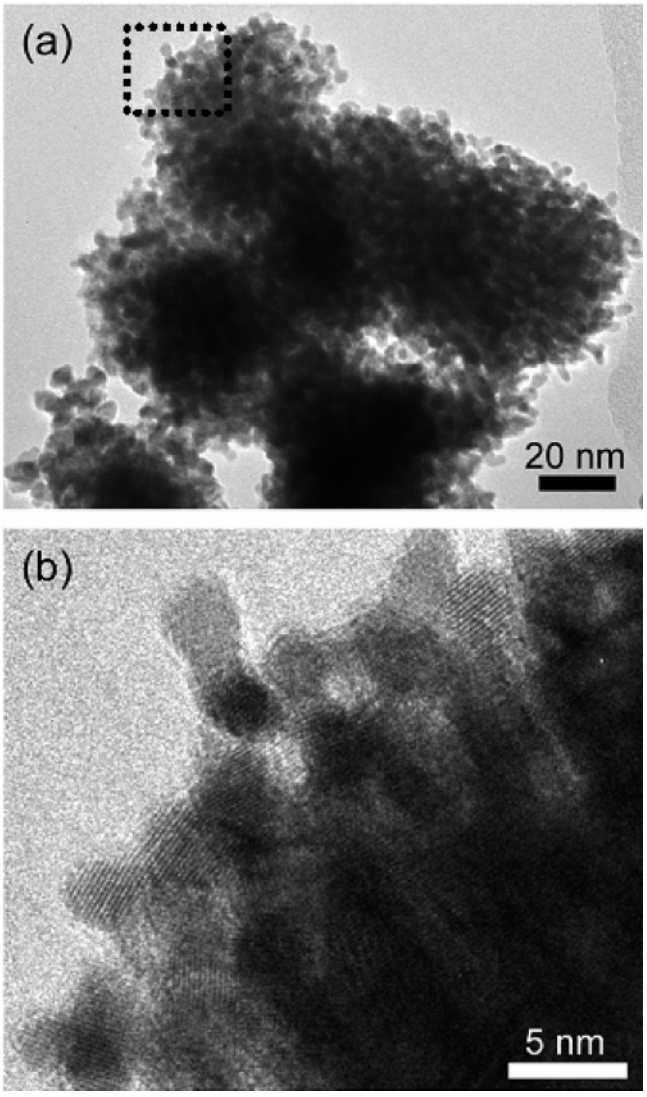

Figure 4. (a) TEM images of the morphology of mesoporous Pt prepared with SBH. (b) Highly magnified TEM image of the square area in panel a.

(16) (a) Çelik, Ö.; Dag, Ö. *Angew. Chem., Int. Ed.* **2001**, *40*, 3800−3803. (b) Dag, Ö.; Samarskaya, O.; Tura, C.; Günay, A.; Çelik, Ö. *Langmuir* **2003**, 3671−3676. (c) Dag, Ö.; Alayoglu, S.; Uysal, I. *J. Phys. Chem. B* **2004**, *108*, 8439−8446.

(17) (a) Nagy, J. B.; Lufimpadio, N.; Gourgue, A.; Derouane, E. G., *Abstr. Pap.*—Am. Chem. *Soc.* **1983**, *185*, 131. (b) Lufimpadio, N.; Gourgue, A.; Nagy, J. B.; Derouane, E. G. *Bull. Soc. Chim. Belg.* **1982**, *91*, 479. (c) Nakanishi, T.; Iida, H.; Osaka, T. *Chem. Lett.* **2003**, *32*, 1166−1167.

Conclusion

Meso-Pt prepared by direct physical casting has specific structural features. The frameworks are composed of connected Pt nanoparticles of ca. 3 nm in size. The lattice fringes on the atomic crystallinity in the frameworks are coherently extended across several nanoparticles. The accurate structural information obtained in this study is very important with regard to the various properties, including electrochemical and catalytic performances as well as thermal and mechanical stabilities, and will be highly useful for future metal deposition within the limited aqueous domains. Mesoporous metals prepared through direct physical casting from H_I-LLC phases consist of a 2D hexagonal *p6 mm* structure with an ordered hexagonal array of one-dimensional channels. Importantly, such a structure is not attainable by the previous replication method with mesoporous silica. The advantage of the LLC templating method is the simple one-pot process of ordered mesoporous metal with good crystallinity, and this study provides another example of mesoporous materials with crystallike wall structures.[18]

Acknowledgment. We greatly thank Dr. T. Yokoshima (National Institute of Advanced Industrial Science and Technology, AIST) for valuable discussion on Pt deposition in the presence of LLC. Advice from Dr. T. Itagaki is also appreciated. O.T. thanks the Swedish Research Council (VR) for support. This work was supported in part by a Grant-in-Aid for Center of Excellence (COE) Research Molecular Nano-Engineering, the 21st Century COE Program Practical Nano-Chemistry, and by the Encouraging Development Strategic Research Centers program Establishment of Consolidated Research Institute for Advanced Science and Medical Care from the Ministry of Education, Culture, Sports, Science and Technology (MEXT), Japanese government.

CM051844Q

(18) (a) Yang, P. D.; Zhao, D. Y.; Margolese, D. I.; Chmelka, B. F.; Stucky, G. D. *Nature* **1998**, *396*, 152−155. (b) Liu, Y.; Zhang, W. Z.; Pinnavaia, T. J. *Angew. Chem., Int. Ed.* **2001**, *40*, 1255−1258. (c) Lee, B.; Lu, D. L.; Kondo, J. N.; Domen, K. *Chem. Commun.* **2001**, 2118−2119. (d) Inagaki, S.; Guan, S.; Ohsuna, T.; Terasaki, O. *Nature* **2002**, *416*, 304−307. (e) Katou, T.; Lee, B.; Lu, D. L.; Kondo, J. N.; Hara, M.; Domen, K. *Angew. Chem., Int. Ed.* **2003**, *42*, 2382−2385. (f) Li, D. L.; Zhou, H. S.; Honma, I. *Nat. Mater.* **2004**, *3*, 65−72.